Formation of $[b_{(n-1)} + OH + H]^+$ Ion Structural Analogs by Solution-Phase Chemistry

Joshua S. Sharp and Kenneth B. Tomer
Laboratory of Structural Biology, National Institute of Environmental Health Sciences,
National Institutes of Health, Research Triangle Park, North Carolina, USA

Derivatization of a variety of peptides by a method known to enhance anhydride formation is demonstrated by mass spectrometry to yield ions that have elemental composition and fragmentation properties identical to $[b_{(n-1)} + OH + H]^+$ ions formed by gas-phase rearrangement and fragmentation. The $[b_{(n-1)} + OH + H]^+$ ions formed by gas-phase rearrangement and fragmentation and the solution-phase $[b_{(n-1)} + OH + H]^+$ ion structural analogs formed by derivatization chemistry show two different forms of dissociation using multiple-collision CAD in a quadrupole ion trap and unimolecular decomposition in a TOF-TOF; one group yields identical product ions as a truncated form of the peptide with a free C-terminal carboxylic acid and fragments at the same activation energy; the other group fragments differently from the truncated peptide, being more resistant to fragmentation than the truncated peptide and yielding primarily the $[b_{(n-2)} + OH + H]^+$ product ion. Nonergodic electron capture dissociation MS/MS suggests that any structural differences between the specific-fragmenting $[b_{(n-1)} + OH + H]^+$ ions and the truncated peptide is at the C-terminus of the peptide. The specific-fragmentation can be readily observed by MS^n experiments to occur in an iterative fashion, suggesting that the C-terminal structure of the original $[b_{(n-1)} + OH + H]^+$ ion is maintained after subsequent rearrangement and fragmentation events in peptides which fragment specifically. A mechanism for the formation of specific-fragmenting and nonspecific-fragmenting $[b_{(n-1)} + OH + H]^+$ ions is proposed.   (J Am Soc Mass Spectrom 2005, 16, 607–621) © 2005 American Society for Mass Spectrometry

Tandem mass spectrometry is a popular tool for the characterization of the primary structure of peptides [1]. Much effort has been directed toward the elucidation of the mechanisms of peptide fragmentation in the gas phase, and a number of reviews on the subject are available [2–4]. Some details about the mechanism of fragmentation and the structures of the fragmentation products have been elucidated [5–9]. For the past fifteen years, considerable effort has gone into the understanding of the structure peptide rearrangement ions and the mechanisms that drive these rearrangements [10–18]. One of the major areas of interest has been the $[b_{(n-1)} + OH + Cat]^+$ ion, which has been observed in a variety of peptides with a variety of cations using a variety of different ionization techniques and mass analyzers [12–14, 16–23]. Understanding the structure of these rearrangement ions and their mechanisms of formation is important for the analysis of peptide tandem mass spectra, as well as for helping to elucidate the general principles of peptide fragmentation.

Isotopic labeling studies of the $[b_{(n-1)} + OH + H]^+$ ion of bradykinin showed that the ion retains the C-terminal oxygen atom, while losing the rest of the C-terminal residue. Based on this result, as well as on a fragmentation study of the $[b_{(n-1)} + OH + H]^+$ ion of bradykinin compared with that of *des*-Arg^9-bradykinin, the structure of the $[b_{(n-1)} + OH + H]^+$ ion was hypothesized to be identical to that of the truncated peptide, i.e., a free acid C-terminus [12]. Multiple groups have proposed a mechanism for the formation of the $[b_{(n-1)} + OH + H]^+$ that involves the initial formation of a seven-membered hydrogen-bonded ring at the neutral C-terminus, followed by collapse into a five-membered cyclic anhydride, which then results in loss of the C-terminal amino acid residue with retention of the original C-terminal oxygen at the new C-terminal free acid (Scheme 1) [12, 13]. Two important features of this mechanism should be noted—the initial formation of a five-membered cyclic anhydride and the free carboxylic acid C-terminus of the end product.

Recently, Farrugia and O'Hair reported the results of experimentation and computational modeling of
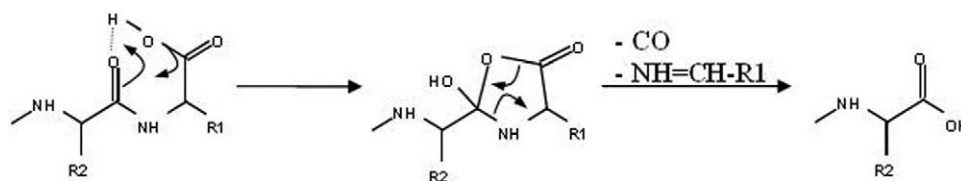
Scheme 1

gas-phase rearrangements of Arg-Gly and Gly-Arg dipeptides [17]. Their work strongly suggests that the rearrangement in these peptides to form the $[b_{(n-1)} + OH + H]^+$ ion goes through a five-membered cyclic intermediate (this time initiated from zwitterions at the N- and C-termini as opposed to the neutral termini proposed earlier) that then becomes a linear anhydride, the actual species that leads to fragment ions (Scheme 2). Once again, the formation of the five-membered cyclic anhydride is a key step in the rearrangement process. Feng et al. suggest in their studies of dipeptide-metal ion complexes that the resulting $[b_{(n-1)} + OH + M]^+$ fragments have free carboxylic acid C-termini [16], and Farrugia and O'Hair support this conclusion in their report [17].

All mechanisms proposed thus far result in a $[b_{(n-1)} + OH + H]^+$ ion with a free acid C-terminus. However, an earlier report by Thorne and Gaskell examining the fragmentation characteristics of the $[b_{(n-1)} + OH + H]^+$ ion of angiotensin III showed that the peptide did not fragment in a standard manner. In fact, the only significant fragmentation product in the MS³ fragmentation of the $[b_{(n-1)} + OH + H]^+$ ion is the $[b_{(n-2)} + OH + H]^+$ ion [19]. Thorne and Gaskell suggested that this fragmentation pattern may be analogous to that noted for metal-cationized peptides [20]; however, it was never explained why the $[b_{(n-1)} + OH + H]^+$ ion of angiotensin III fragmented only to the $[b_{(n-2)} + OH + H]^+$ ion, while the $[b_{(n-1)} + OH + H]^+$ ion of bradykinin fragmented nonspecifically.

In order to test the proposed mechanisms for the fragmentation events involved in the formation of $[b_{(n-1)} + OH + H]^+$ ions, a method was developed to synthesize structures that have elemental compositions and fragmentation characteristics identical to those of $[b_{(n-1)} + OH + H]^+$ ions formed by gas-phase rearrangement and fragmentation. The chemistry that yields such an analog should give significant insights into the structure of the $[b_{(n-1)} + OH + H]^+$ ion. In addition, the ability to make peptide analogs that are

structurally identical to $[b_{(n-1)} + OH + H]^+$ ions should allow a variety of analytical techniques, such as NMR and FT-IR, to be brought to bear in studying the structure of these ions. The fragmentation properties and elemental composition of these solution-phase products (as well as their gas-phase analogs) were then compared to peptides lacking the C-terminal residue to determine if the $[b_{(n-1)} + OH + H]^+$ product ions have the same structure as the truncated peptide with a free C-terminal carboxylic acid as previously proposed [12, 13, 16, 17].

Experimental

All peptides used were obtained from Sigma-Aldrich (St. Louis, MO) except for LWMRFA, *des*-Arg⁹-bradykinin, and *des*-Leu¹⁰-angiotensin I (Bachem Bioscience, King of Prussia, PA) and used without further purification. All reagents were obtained from Sigma-Aldrich and used without further purification unless otherwise noted.

Solution-Phase Formation of $[b_{(n-1)} + OH + H]^+$ Ion Structural Analogs

Solution-phase $[b_{(n-1)} + OH + H]^+$ ion structural analogs (hereafter termed $[b_{(n-1)} + OH + H]_S^+$ ions) were generated by modification of the protocol of Hardeman et al. for formation of C-terminal oxazolinones [24]. Peptides were weighed out and suspended at a concentration of 0.185 mg peptide/ml in acetic anhydride (AcAn) with 7.4% trifluoroacetic acid (Pierce Biotechnology, Rockford, IL). The peptide mixture was heated at 55 °C for 15 to 25 minutes with gentle mixing. Following the incubation, the solution was dried to completeness by vacuum centrifuge and resuspended in acetonitrile with 0.1% formic acid for mass spectrometric analysis. For formation of acetylated peptides for comparison of gas-phase $[b_{(n-1)} + OH + H]^+$ ions by
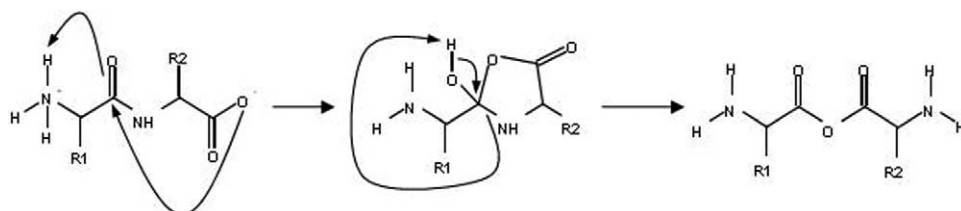
Scheme 2

MS^n, the same protocol was followed except no trifluoroacetic acid (TFA) was used. No solution-phase $[b_{(n-1)} + OH + H]^+$ ion structural analogs were detected in the absence of TFA in the reaction.

MALDI-TOF-TOF Mass Spectrometry

All matrix assisted laser desorption ionization-time of flight-time of flight (MALDI-TOF-TOF) spectra were obtained on an Applied Biosystems (Foster City, CA) 4700 Proteomics Analyzer instrument. A spot of 0.2 μl of a 33% saturated solution of recrystallized α-cyano-4-hydroxycinnamic acid in 50% methanol, 50% water with 0.1% formic acid was spotted onto a stainless steel target. A 0.2 μl spot of peptide was added to the matrix droplet and allowed to cocrystallize. The MALDI-TOF-TOF instrument was operated in the positive ionization, reflector mode. Tandem mass spectrometry (MS/MS) spectra were obtained by post-source decay with the collision cell at background pressure ($\sim$1.5 $\times$ 10^{-8} torr), and a 1 kV ion acceleration voltage. All MS/MS spectra used for direct comparison were taken under the exact same conditions at approximately the same time in order to maximize experimental comparability.

MALDI-FT-ICR Mass Spectrometry

All Fourier transform-ion cyclotron resonance (FT-ICR) mass spectrometry was performed using a 9.4 T, actively shielded IonSpec FTMS (Lake Forest, CA).

MALDI-FT-ICR transient acquisitions were performed in the broadband mode. Matrix was prepared by adding 150 mg of 2,5-dihydroxybenzoic acid (Sigma-Aldrich) to 1 ml of a solution of 50% methanol (Mallinckrodt Laboratory Chemicals, Phillipsburg, NJ) and 50% deionized water filtered in-house. Matrix solution (0.3 μl) was pipetted onto the stainless steel target. Peptide solution (0.3 μl) was pipetted on top of the still-wet matrix droplet and allowed to cocrystallize. The sample was irradiated with a Nd:YAG laser at 355 nm. Nitrogen was pulsed in to the analyzer cell to cool the ions prior to analysis, and a delay of 8 s was used to allow the analyzer cell to pump down to a pressure of $\sim$8 $\times$ 10^{-10} torr prior to signal acquisition. Spectra were internally calibrated, resulting in a mass error less than 2 ppm. Elemental composition analyses were performed using the IonSpec Elemental Composition package. Between 2 and 30 spectra were obtained and averaged, depending on the signal intensity of the ion(s) of interest.

ESI-FT-ICR Electron Capture Dissociation Tandem Mass Spectrometry

A nanoelectrospray source (Micromass Milford, MA) was used in all ESI-FT-ICR experiments. Analyte was dissolved in acetonitrile with 1% formic acid was infused by syringe pump at a flow rate of 500 nl/min,

with a probe voltage of 3.8 kV. Ions were accumulated in an external hexapole [25] for a period of 3 s before injection into the analyzer cell. Electron capture dissociation (ECD) analysis was performed by a method similar to those previously reported [26, 27]. Ions of interest for ECD analysis were isolated in the analyzer cell. A voltage of 4.5 V was applied to a dispenser cathode for the duration of the experiment. A voltage of −0.56 V was applied opposite the analyzer cell to force the electrons into proximity with the analyte ions. A total of ten scans were averaged for each spectrum, with 256 K data points collected across a 256 ms transient.

ESI-QIT Mass Spectrometry

All ESI-quadrupole ion trap (QIT) spectra were obtained using an Agilent Technologies (Palo Alto, CA) LC/MSD Trap XCT mass spectrometer operated in the positive ion mode at a flow rate of 2 μl/min. The ESI probe was held at ground potential, while the capillary was operated at −3.5 kV, and helium bath gas was used for collision in all collisionally activated dissociation (CAD) MS/MS experiments at a pressure of 8 $\times$ 10^{-6} torr. For all CAD MS/MS experiments, the SmartFrag option was turned off. A fragmentation delay of 20 ms, a fragmentation time of 40 ms, and an m/z precursor isolation width of 10 m/z were used for fragmentation of angiotensin I analogs; a fragmentation delay of 0 ms, a fragmentation time of 40 ms, and an m/z precursor isolation width of 10 m/z were used for fragmentation of bradykinin analogs. Instrument parameters remained identical for all angiotensin analog experiments; likewise, all instrument settings for the bradykinin analog experiments were identical.

Results and Discussion

In order to generate solution-phase structural analogs to $[b_{(n-1)} + OH + H]^+$ ions by solution-phase chemistry, a modification of a method for the generation of C-terminal oxazolinones [24] was utilized. A MALDI-TOF spectrum of one such reaction using Ile[7] angiotensin III (peptide sequence RVYIHPI) is shown in Figure 1. The loss of 113 Da from the initial reactant mass, along with various acetylations [Ac] and/or trifluoroacetylations [F$_3$Ac], explain all major ions in the spectrum. Also, the ions of m/z 826, 868, 880, and 922 all fragmented in a similar manner, resulting primarily in a loss of 97 Da (described in detail below), while the ions of m/z 993 and 1035 yielded b- and y-type fragment ions consistent with Ile[7] angiotensin III. These data suggest that the four ions of m/z 826, 868, 880, and 922 are structurally related. The ions of m/z 944 and 960 also fragmented to yield primarily a loss of 97 Da; however, these ions correspond to sodiated and potassiated ions which are known to undergo metal-induced fragmentation/rearrangement reactions [14, 16, 22, 23]. The ion corresponding in mass to the nonacetylated $[b_6 + OH + H]_S^+$ analog of Ile[7] angiotensin III was not present in
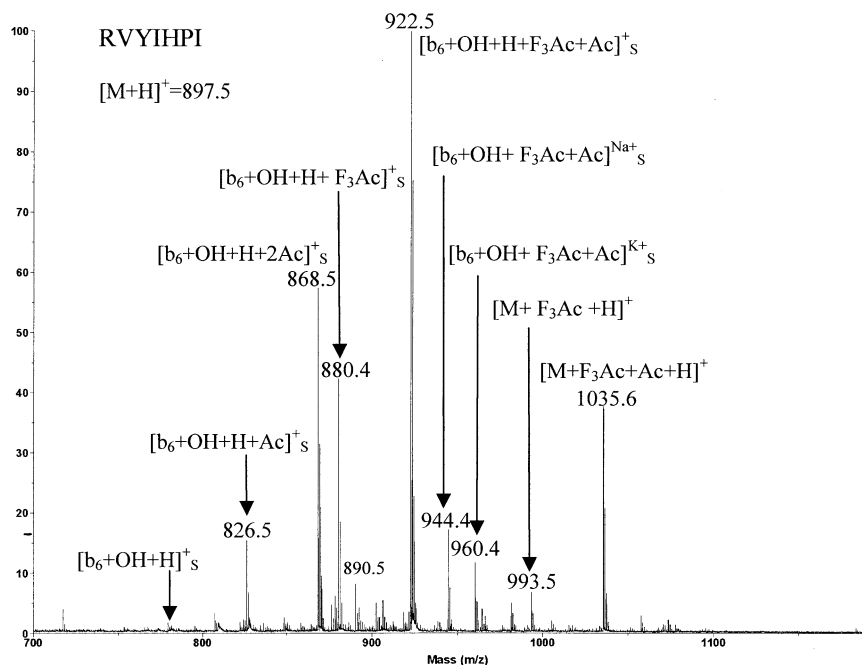
Figure 1. MALDI-TOF spectrum of products of Ile^7 angiotensin III from the AcAn:TFA reaction. Abundant ions matching the mass of acetylated and trifluoroacetylated peptide minus isoleucine are tentatively labeled as $[b_6 + OH + H]_s^+$ ions. Present barely above the noise is the unacetylated $[b_6 + OH + H]_s^+$ ion.

sufficient abundance to isolate and fragment by MS/MS. In order to ensure that the observed ions were not products of in-source fragmentation, the MALDI-TOF experiment was repeated under the same conditions for untreated Ile^7 angiotensin III peptide and the peptide treated only with acetic anhydride, which leads to extensive acetylation. In both cases, ions corresponding

to a loss of isoleucine were not detected (data not shown).

In order to verify that the masses of the solution-phase reaction products measured here are indeed indicative of loss of Ile from various acetylated and/or trifluoroacetylated starting material, exact mass measurements of the reaction products were acquired using

Table 1. Exact mass calculations for observed solution-phase $[b_{(n-1)} + OH + H]_s^+$ ion structural analogs

Observed m/z = 868.4666 ± 0.002			Observed m/z = 880.4272 ± 0.002			Observed m/z = 922.4384 ± 0.002		
Number of Fluorines = 0			Number of Fluorines = 3			Number of Fluorines = 3		
m/z	Delta m/z	Formula	m/z	Delta m/z	Formula	m/z	Delta m/z	Formula
868.46673	−0.00013	$H_{62}C_{25}O_{15}N_{19}$	880.42739	−0.00019	$H_{55}C_{37}O_8N_{14}F_3$	922.43847	−0.00007	$H_{59}C_{25}O_{15}N_{19}F_3$
868.46674	−0.00014	$H_{68}C_{26}O_{20}N_{12}$	880.42740	−0.00020	$H_{61}C_{38}O_{13}N_7F_3$	922.43847	−0.00007	$H_{65}C_{26}O_{20}N_{12}F_3$
868.46624	0.00036	$H_{72}C_{41}O_{19}$	880.42741	−0.00021	$H_{67}C_{39}O_{18}F_3$	922.43879	−0.00039	$H_{57}C_{55}O_4N_6F_3$
868.46623	0.00037	$H_{66}C_{40}O_{14}N_7$	880.42689	0.00031	$H_{59}C_{52}O_7N_2F_3$	922.43797	0.00043	$H_{69}C_{41}O_{19}F_3$
868.46622	0.00038	$H_{60}C_{39}O_9N_{14}$	880.42688	0.00032	$H_{53}C_{51}O_2N_9F_3$	922.43796	0.00044	$H_{63}C_{40}O_{14}N_7F_3$
868.46706	−0.00046	$H_{60}C_{55}O_4N_6$	880.42657	0.00063	$H_{61}C_{22}O_{18}N_{15}F_3$	922.43796	0.00044	$H_{57}C_{39}O_9N_{14}F_3$
868.46572	0.00088	$H_{64}C_{54}O_8N_2$	880.42790	−0.00070	$H_{57}C_{23}O_{14}N_{19}F_3$	922.43929	−0.00089	$H_{53}C_{40}O_5N_{18}F_3$
868.46571	0.00089	$H_{58}C_{53}O_3N_9$	880.42791	−0.00071	$H_{63}C_{24}O_{19}N_{12}F_3$	922.43930	−0.00090	$H_{59}C_{41}O_{10}N_{11}F_3$
868.46756	−0.00096	$H_{56}C_{40}O_5N_{18}$	880.42822	−0.00102	$H_{55}C_{53}O_3N_6F_3$	922.43931	−0.00091	$H_{65}C_{42}O_{15}N_4F_3$
868.46757	−0.00097	$H_{62}C_{41}O_{10}N_{11}$	880.42606	0.00114	$H_{65}C_{37}O_{17}N_3F_3$	922.43745	0.00095	$H_{61}C_{54}O_8N_2F_3$
868.46757	−0.00097	$H_{68}C_{42}O_{15}N_4$	880.42606	0.00114	$H_{59}C_{36}O_{12}N_{10}F_3$	922.43745	0.00095	$H_{55}C_{53}O_3N_9F_3$
868.46540	0.00120	$H_{66}C_{24}O_{19}N_{15}$	880.42605	0.00115	$H_{53}C_{35}O_7N_{17}F_3$	922.43713	0.00127	$H_{63}C_{24}O_{19}N_{15}F_3$
868.46808	−0.00148	$H_{64}C_{27}O_{16}N_{16}$	880.42873	−0.00153	$H_{51}C_{38}O_4N_{18}F_3$	922.43981	−0.00141	$H_{61}C_{27}O_{16}N_{16}F_3$
868.46489	0.00171	$H_{70}C_{39}O_{18}N_3$	880.42873	−0.00153	$H_{57}C_{39}O_9N_{11}F_3$	922.44013	−0.00173	$H_{53}C_{56}N_{10}F_3$
868.46489	0.00171	$H_{64}C_{38}O_{13}N_{10}$	880.42874	−0.00154	$H_{63}C_{40}O_{14}N_4F_3$	922.44013	−0.00173	$H_{59}C_{57}O_5N_3F_3$
868.46488	0.00172	$H_{58}C_{37}O_8N_{17}$	880.42555	0.00165	$H_{57}C_{50}O_6N_5F_3$	922.43663	0.00177	$H_{67}C_{39}O_{18}N_3F_3$
868.46839	−0.00179	$H_{56}C_{56}N_{10}$	880.42554	0.00166	$H_{51}C_{49}ON_{12}F_3$	922.43662	0.00178	$H_{61}C_{38}O_{13}N_{10}F_3$
868.46840	−0.00180	$H_{62}C_{57}O_5N_3$	880.42522	0.00198	$H_{59}C_{20}O_{17}N_{18}F_3$	922.43661	0.00179	$H_{55}C_{37}O_8N_{17}F_3$

MALDI-FT-ICR. Table 1 shows the result of an elemental composition analysis of three protonated molecules suspected to be attributable to the presence of starting material with various acetylations and/or trifluoroacetylations and the loss of the C-terminal Ile residue. The elemental composition search parameters used were 1 to 100 carbon, hydrogen, oxygen, and nitrogen atoms, and 0 to 9 fluorine atoms (double bond equivalents were disregarded to allow for the broadest practical search). All results that contained fluorine atoms not in a multiple of three were excluded. For the three measured masses examined, a theoretical mass matched the measured mass that was consistent with a shift from the mass of the parent peptide minus the C-terminal Ile ($C_{37}H_{58}N_{11}O_8$) plus (1) two acetylations ($+C_4H_4O_2$), (2) one trifluoroacetylation ($-H, +C_2F_3O$), or (3) one acetylation and one trifluoroacetylation ($+C_4HF_3O_2$). In order to verify the results of the elemental composition analysis, the solution-phase reaction was performed using trichloroacetic acid in place of trifluoroacetic acid, resulting in trichloroacetylations instead of trifluoroacetylations. The number of fluorines in each original derivative was determined by its mass shift in the trichloroacetylated form. In each case, the number of fluorines matched those determined by elemental composition analysis. No other group of three masses was consistent with each other and with the Ile[7] angiotensin III starting material. The ion of m/z 826 was not present in the MALDI-FT-ICR spectrum at sufficient abundance for an exact mass measurement; however, the mass and fragmentation data from the MALDI-TOF-TOF spectrum, as well as the elemental composition assignment of the other three masses of interest, strongly suggest that the ion of m/z 826 is due to loss of the C-terminal Ile from acetylated starting Ile[7] angiotensin III. No ions which could be attributed to loss of other residues in the peptide were observed in this MALDI-TOF spectrum; the loss of the C-terminal isoleucine residue seemed to be specific.

An early observation was made that upon activation by MALDI-TOF-TOF at 1 kV acceleration potential with no collision gas added, some solution-phase $[b_{(n-1)} + OH + H]_S^+$ ion structural analogs rearranged and fragmented into the $[b_{(n-2)} + OH + H]^+$ product ion as their most preferred fragmentation pathway (hereafter termed "specific-fragmenting"). In contrast, the most preferred fragmentation pathway for other solution-phase $[b_{(n-1)} + OH + H]_S^+$ ion structural analogs were into more standard b- or y-type ions, with the $[b_{(n-2)} + OH + H]^+$ fragment ion present but not representing the most favored fragmentation pathway (hereafter termed "nonspecific-fragmenting"). For example, the MALDI-TOF-TOF MS/MS spectrum of the solution-phase generated $[b_6 + OH + H]_S^+$ ion structural analog of Ile[7] angiotensin III (peptide sequence RVYIHPI) with an N-terminal trifluoroacetylation and acetylation [Ac] of the Tyr[3] sidechain (m/z 922 and labeled as $[b_6 + OH + H + F_3Ac + Ac]$ in Figure 1) obtained by unimolecular decomposition is shown in Figure 2a. The proton-

ated molecule of the $[b_6 + OH + H]_S^+$ ion structural analog of Ile[7] angiotensin III (m/z 922.4) fragmented in a specific manner, yielding primarily the $[b_5 + OH + H]^+$ ion of m/z 825.4, with the $[b_4 + OH + H]^+$ ion and some standard a- and b-type ions present at relatively low abundance. Similar fragmentation patterns for the $[b_{(n-1)} + OH + H]^+$ ion of angiotensin III and the $[b_{(n-1)} + OH + Na]^+$ ion of methionine enkephalin in MS[3] experiments were previously reported by Thorne and Gaskell, where the $[b_{(n-2)} + OH + Cat]^+$ ion was the only significant fragmentation product observed [19]. Under the same fragmentation conditions used for the experiment above, the MS/MS spectrum of the protonated molecule of full-length acetylated, trifluoroacetylated Ile[7] angiotensin III (Figure 1, m/z 1035.6) yields mainly b- and a-type fragment ions, with no detectable $[b_5 + OH + H]^+$ fragment product (data not shown). The unimolecular decay MS/MS spectrum of the solution-phase generated $[b_4 + OH + H]_S^+$ ion structural analog of proctolin (peptide sequence RYLPT, m/z 632.1), with an N-terminal acetylation and Tyr[2] sidechain acetylation, is shown in Figure 2b. In contrast to the MS/MS spectrum of the solution-phase generated $[b_{(n-1)} + OH + H]_S^+$ ion structural analog of Ile[7] angiotensin III (m/z 922.4) shown in Figure 2a, the fragmentation of this $[b_4 + OH + H + 2Ac]_S^+$ ion analog of proctolin yields $[b_3 + OH + H]^+$ fragment ion of m/z 535.5 at a relative abundance of ~47%, but the most abundant fragment ion is a b_2-NH$_3$ ion, with many other abundant b- and a-type ions present. This fragmentation pattern is quite similar to diacetylated full length proctolin. Solution-phase generated $[b_{(n-1)} + OH + H]_S^+$ ion structural analogs of proctolin fragmented in this nonspecific fashion regardless of acetylation or trifluoroacetylation in all cases examined (data not shown).

In order to determine if the observed differences between fragmentation pathways reported here, as well as those previously reported [12, 19], are generally applicable, we attempted to form the solution-phase $[b_{(n-1)} + OH + H]_S^+$ ion structural analogs from a variety of peptides. A list of the peptides which were successfully derivatized is shown in Table 2. For the peptides studied, two factors were determined to be necessary for the successful formation and detection of the solution-phase $[b_{(n-1)} + OH + H]_S^+$ ion structural analog: first, the peptide must have a free acid C-terminus; second, the peptide must have either a histidine or arginine side chain. The need for a free acid C-terminus has been previously reported for formation of the gas-phase $[b_{(n-1)} + OH + H]^+$ ion [12]. The need for a histidine or arginine side chain is probably not necessary for the chemistry; rather, due to the high amount of acetylation that occurs under these reaction conditions, a basic side chain that is resistant to acetylation is probably necessary for ionization in the positive mode. Peptide $[b_{(n-1)} + OH + H]_S^+$ ion structural analogs that demonstrated a propensity to fragment and rearrange to the $[b_{(n-2)} + OH + H]^+$ ion in
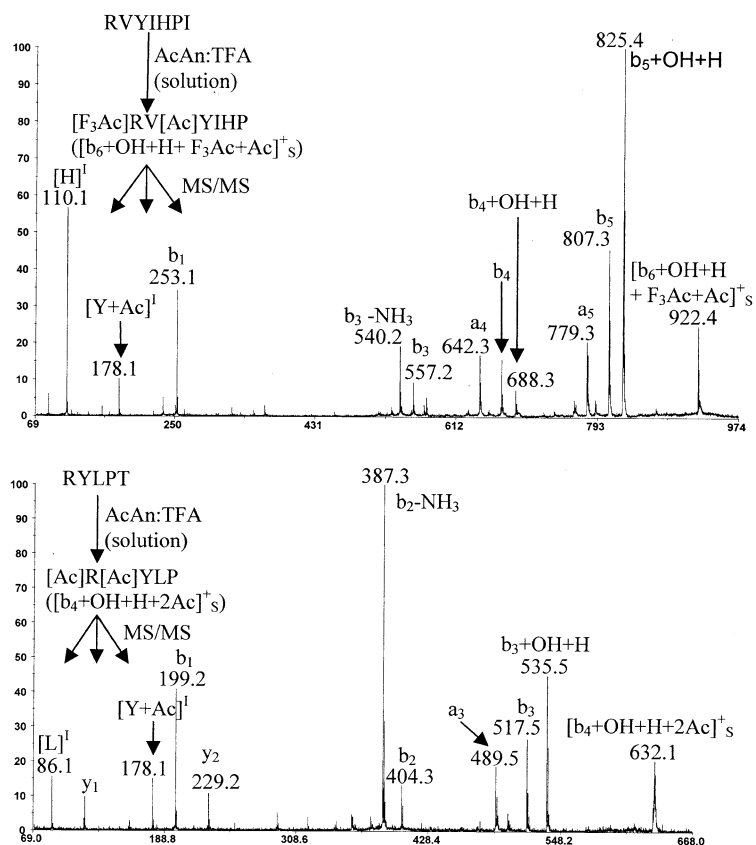
Figure 2. (**a**) MALDI-TOF-TOF MS/MS spectrum of the solution-phase $[b_6 + OH + H]_S^+$ ion structural analog of N-terminally trifluoroacetylated, tyrosine acetylated Ile^7 angiotensin III. The most abundant fragment ion is the $[b_5 + OH + H]^+$ ion of m/z 825.4. (**b**) MALDI-TOF-TOF MS/MS spectrum of the solution-phase $[b_4 + OH + H]_S^+$ ion structural analog of diacetylated proctolin. The $[b_3 + OH + H]^+$ ion of m/z 535.5 is present, but the most abundant fragmentation product is the b_2-NH_3 ion of m/z 387.3.

preference to any other product ion when fragmented by MALDI-TOF-TOF at a 1 kV acceleration potential with no collision gas added (as determined by the most abundant product ion in the MS/MS spectra) were labeled "specific" fragmenting. Peptide $[b_{(n-1)} + OH + H]_S^+$ ion structural analogs that demonstrated a propensity to preferentially fragment into a product ion other than the $[b_{(n-2)} + OH + H]^+$ ion when fragmented

under the same conditions were labeled "nonspecific" fragmenting. By separating the $[b_{(n-1)} + OH + H]_S^+$ ion structural analogs based on their most preferred fragmentation pathway, the structures of the peptides can be examined for features that promote further rearrangement of the $[b_{(n-1)} + OH + H]^+$ ion into the $[b_{(n-2)} + OH + H]^+$ ion. No immediately obvious structural correlations were observed between the spe-

Table 2. Fragmentation patterns of successfully-formed solution-phase $[b_{(n-1)}+OH + H]^+s$ ion structural analogs

Name	Sequence	Fragmentation pattern
LWMRFA	LWMRFA	Specific
[Sar^1, Gly^8] angiotensin II	Sar-RVYIHPG	Specific
[Sar^1] angiotensin II	Sar-RVYIHPF	Specific
angiotensin I	DRVYIHPFHL	Specific
[Val^5] angiotensin I	DRVYVHPFHL	Specific
[Ile^7] angiotensin III	RVYIHPI	Specific
Proctolin	RYLPT	Nonspecific
Neurotensin	pyroGlu-LYENKPRRPYIL	Nonspecific
HPFHLdLVY	HPFHLdLVY	Nonspecific
PHPFHLFVY	PHPFHLFVY	Nonspecific
Bradykinin	RPPGFSPFR	Nonspecific
des-Arg^1-bradykinin	PPGFSPFR	Nonspecific
des-Arg^9-bradykinin	RPPGFSPF	Nonspecific

cific and nonspecific-fragmenting peptides. All specific-fragmenting peptides contained at least one arginine, but this observation could be coincidence, because of the low number of histidine-containing, arginine-free peptides examined. A peptide with an N-terminal secondary amine was found in both the specific-fragmenting (N-terminal sarcosine) and the nonspecific-fragmenting (N-terminal pyroglutamate) peptides. Both categories had peptides with N-terminal arginines, but neither required an N-terminal arginine. Other than the two previously-mentioned requirements, no conclusions could be reached from this tabulation.

To this point, the exact mass measurement and MS/MS fragmentation data suggest that we are reproducing the $[b_{(n-1)} + OH + H]^+$ ion structure by solution-phase chemistry to form an exact structural analog to the gas-phase rearrangement and fragmentation product; however, a more direct correlation between the structure of the solution-phase generated $[b_{(n-1)} + OH + H]_S^+$ ion structural analog and the gas-phase $[b_{(n-1)} + OH + H]^+$ rearrangement and fragmentation product ion must be established before the analog can be used as a model of gas-phase $[b_{(n-1)} + OH + H]^+$ ion structure. In order to do so, the MS/MS spectra of the gas-phase $[b_{(n-1)} + OH + H]^+$ rearrangement and fragmentation product ion, the solution-phase generated $[b_{(n-1)} + OH + H]_S^+$ ion structural analog, and a C-terminally truncated peptide with the same sequence were compared. Figure 3 shows a comparison between the fragmentation spectra of the gas-phase $[b_8 + OH + H]^+$ rearrangement fragment ion formed by MS/MS of diacetylated bradykinin (peptide sequence RPPGFSPFR, Figure 3a), the solution-phase diacetylated $[b_8 + OH + H]_S^+$ ion structural analog formed from bradykinin by the solution-phase chemistry described above (Figure 3b), and the diacetylated *des*-Arg[9]-bradykinin truncated peptide (Figure 3c). Figure 3a shows the MS/MS/MS spectrum of diacetylated bradykinin. For analysis of the structure of the gas-phase generated $[b_{(n-1)} + OH + H]^+$ ion of bradykinin, the singly-protonated molecule of diacetylated bradykinin was initially fragmented in the QIT, and the $[b_8 + OH + H]^+$ fragment ion of m/z 988 was isolated and fragmented in an MS/MS/MS experiment at a collision potential of 1.8 V. The most abundant fragment ion observed in the MS[3] spectrum is the y_7 ion; the $[b_7 + OH + H]^+$ ion of m/z 841 is also detected, but at significantly lower relative abundance (~25%). Figure 3b shows the MS/MS spectrum of the diacetylated solution-phase $[b_8 + OH + H]_S^+$ bradykinin structural analog acquired at a collision potential of 1.8 V. The product ion spectrum is virtually identical to that of the gas-phase formed $[b_8 + OH + H]^+$ ion (Fig 3a), with the y_7 fragment ion the most abundant fragment ion detected. Comparison of the two fragmentation spectra strongly supports the proposition that the solution-phase formed $[b_8 + OH + H]_S^+$ ion structural analog is structurally identical to the gas-phase formed $[b_8 + OH + H]^+$ ion. Figure 3c shows the MS/MS spectrum of

diacetylated *des*-Arg[9]-bradykinin acquired at a collision potential of 1.8 V. The product ion spectrum of the truncated peptide is virtually identical to the spectra of the gas-phase $[b_8 + OH + H]^+$ ion and the solution-phase formed $[b_8 + OH + H]_S^+$ ion structural analog, with the y_7 fragment ion as the base peak, and various b- and y-type ions present at lower abundance. Product ions resulting from a loss of 60 Da from the protonated molecule or from a fragment ion are also present at considerable abundance in the fragmentation spectra of all three peptides. Close examination of the fragmentation spectra reveal that all fragment ions that demonstrate the 60 Da loss contain Ser[6], which is known to be acetylated. In addition, no appreciable loss of 18 Da (H_2O) or 42 Da (HN = C = NH) from the protonated molecule is detected, and no carboxylic acid group is adjacent to an arginine to allow for the previously-described loss of the arginine side chain [15, 28]. These observations lead to the assignment of the 60 Da losses to be loss of acetic acid from the Ser[6] side chain. The identical fragmentation spectra of the solution-phase diacetylated $[b_8 + OH + H]_S^+$ ion structural analog of bradykinin, the gas-phase $[b_8 + OH + H]^+$ fragment ion of diacetylated bradykinin, and the diacetylated *des*-Arg[9]-bradykinin support the hypothesis that the structure of $[b_{(n-1)} + OH + H]^+$ ions is identical to that of the truncated peptide [12, 13, 17]. The observation that the gas-phase formed $[b_8 + OH + H]^+$ ion fragments similarly to the truncated *des*-Arg[9]-bradykinin was reported previously, and was one of the key points in proposing that the structure of the $[b_{(n-1)} + OH + H]^+$ ion has a free C-terminal carboxylic acid [12].

In addition to bradykinin, the MS/MS spectra of the gas-phase $[b_9 + OH + H]^+$ rearrangement and fragmentation product ion formed from diacetylated angiotensin I (peptide sequence DRVYIHPFHL) by MS/MS, the solution-phase diacetylated $[b_9 + OH + H]_S^+$ ion structural analog formed from angiotensin I by the solution-phase chemistry described above, and a C-terminally truncated diacetylated angiotensin I peptide were compared. The MS/MS/MS spectrum of diacetylated angiotensin I is shown in Figure 4a. Diacetylated angiotensin I was fragmented by CAD, and the $[b_9 + OH + H]^+$ fragment ion (m/z 1267.7) was isolated and fragmented at an activation energy of 1.8 V. The most abundant product ion observed is the $[b_8 + OH + H]^+$ ion of m/z 1130, similar to that observed in the MS/MS spectrum of the solution-phase formed $[b_6 + OH + H]_S^+$ ion structural analog of Ile[7] angiotensin III, m/z 922.4 (Figure 2a). Figure 4b shows the MS/MS spectrum of the solution-phase $[b_9 + OH + H]_S^+$ ion structural analog of diacetylated angiotensin I (m/z 1267.7) acquired at a collision energy of 1.8 V. The product ion spectrum is almost identical to that of the gas-phase formed $[b_9 + OH + H]^+$ ion shown in Figure 4a, again strongly suggesting that the structure of the gas-phase formed $[b_{(n-1)} + OH + H]^+$ ion and the solution-phase $[b_{(n-1)} + OH + H]_S^+$ ion structural analog are identical. Figure 4c shows the MS/MS spectrum of diacetylated
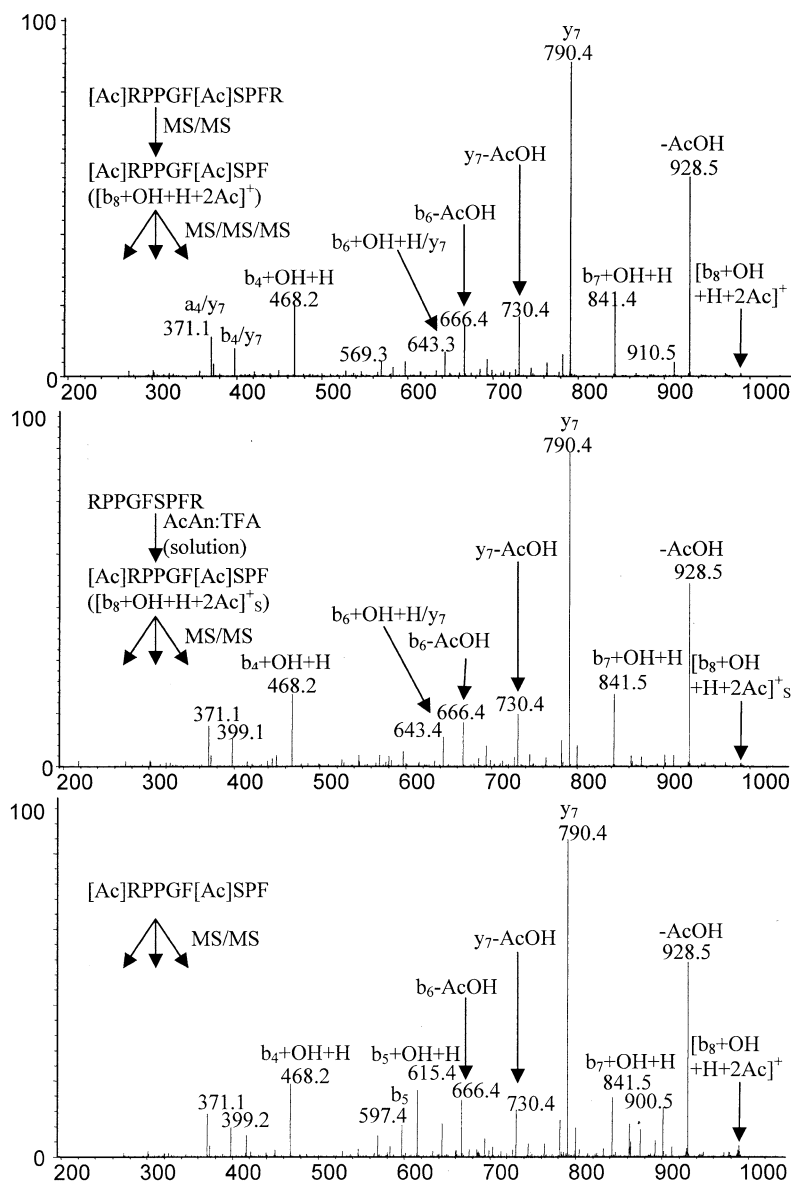
Figure 3. (a) ESI-QIT MS/MS/MS spectrum of diacetylated bradykinin→[b_8 + OH + H]$^+$ ion of diacetylated bradykinin. (b) ESI-QIT MS/MS spectrum of solution-phase generated diacetylated [b_8 + OH + H]^+_S ion structural analog of bradykinin. (c) ESI-QIT MS/MS spectrum of diacetylated *des*-Arg^9-bradykinin. The most abundant fragment in each spectrum is the loss of the N-terminal arginine of *m/z* 790, similar to the MS/MS spectrum of full length diacetylated bradykinin.

des-Leu^{10}-angiotensin I acquired at a collision energy of 1.8 V. The most abundant fragment in this spectrum is the loss of 60 Da. This 60 Da loss is accompanied by losses of 18 Da (H_2O) and 42 Da (HN = C = NH, ion marked with an asterisk), indicative of a side-chain loss from the N-terminal Asp and Arg side chains, similar to the side chain losses frequently observed for C-terminal arginine-containing peptides [15, 28]. This fragment ion resulting from the loss of 60 Da is present at less than 5% relative abundance in the gas-phase [b_9 + OH + H]$^+$ ion and solution-phase [b_9 + OH + H]^+_S ion structural analog fragmentation spectra, indicating that the truncated peptide has a different primary fragmentation pathway than the [b_9 + OH + H]$^+$ ion. These

data strongly suggest that, in at least the case of diacetylated angiotensin I, the structure of the [$b_{(n-1)}$ + OH + H]$^+$ ion is not the same as that of the truncated peptide.

In order to further characterize the solution-phase [$b_{(n-1)}$ + OH + H]^+_S ion structural analog and gas-phase formed [$b_{(n-1)}$ + OH + H]$^+$ ion, we examined the energy of fragmentation for each ion by tandem mass spectrometry in a quadrupole ion trap. In this experiment, the ion of interest was fragmented by MS/MS at different activation voltages, and the ratio of the abundance of fragment ions divided by the total ion abundance was calculated and averaged over one minute. When plotted this way, the data yield a sigmoidal plot,
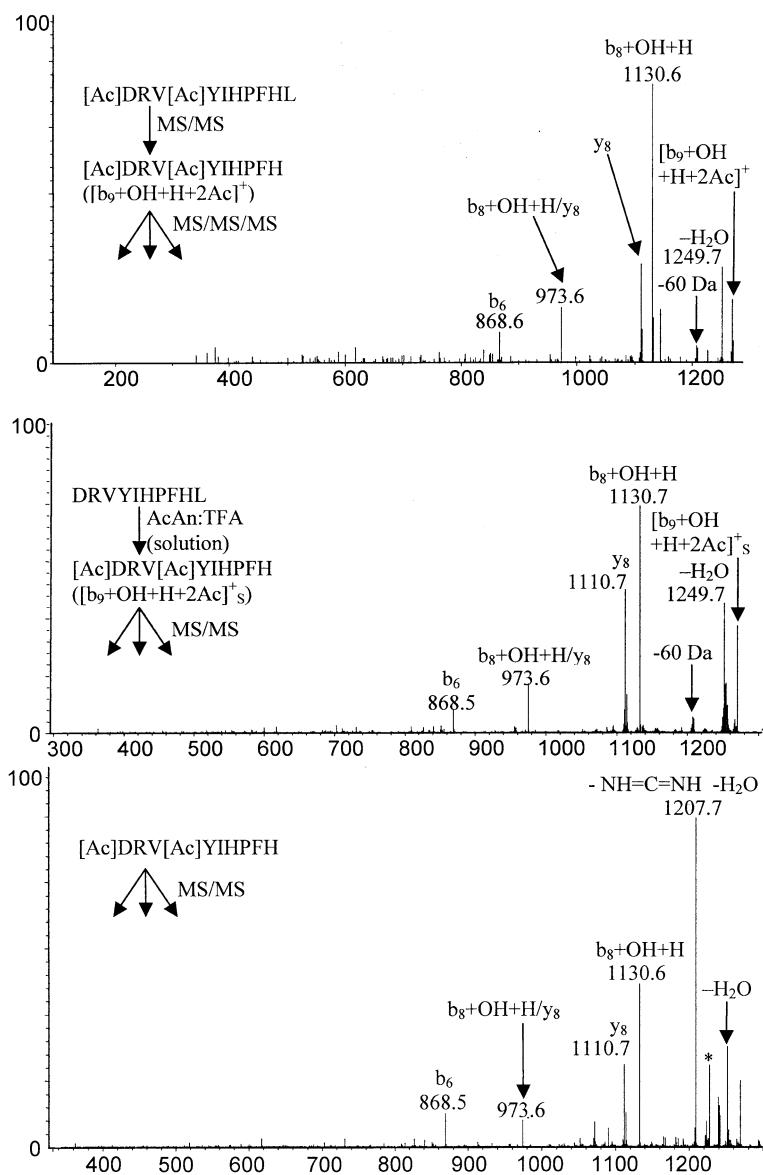
Figure 4. (a) ESI-QIT MS/MS/MS spectrum of diacetylated angiotensin I $\rightarrow$ $[b_9 + OH + H]^+$ ion of diacetylated angiotensin I. (b) ESI-QIT MS/MS spectrum of solution-phase generated diacetylated $[b_9 + OH + H]_S^+$ ion structural analog of angiotensin I. (c) ESI-QIT MS/MS spectrum of diacetylated *des*-Leu^{10}-angiotensin I. The MS/MS spectra of the gas-phase generated $[b_9 + OH + H]^+$ ion and the solution-phase generated structural analog are identical, while the MS/MS spectrum of the truncated peptide is different.

which can be fitted using the Boltzmann equation to find the inflection point situated halfway between the minimum (only parent ion present, with no fragment ion signal above the noise) and the maximum (only fragment ions present, no parent ion signal above the noise). This inflection point, V_{50}, can be compared between species using the same laboratory frame of reference to determine the ease at which an ion fragments. Ions with identical structures will have an identical V_{50}, while ions with different structures will probably have a different V_{50}. In addition, the V_{50} will indicate which ions are more susceptible to fragmentation [29]. As the MS/MS experiments were performed

in a quadrupole ion trap, all MS/MS fragmentations were a result of multiple low-energy collisions; therefore, accuracy in determining the V_{50} value was obtained by careful control of the MS/MS parameters and acquisition of multiple spectra over the one minute time frame. For analysis of the gas-phase generated $[b_{(n-1)} + OH + H]^+$ ions, the $[b_{(n-1)} + OH + H]^+$ rearrangement and fragmentation product was initially formed by MS/MS in the QIT at a fixed voltage, followed by collisional cooling of the product ion in the high-pressure QIT and isolation of the $[b_{(n-1)} + OH + H]^+$ ion for MS^3 analysis.

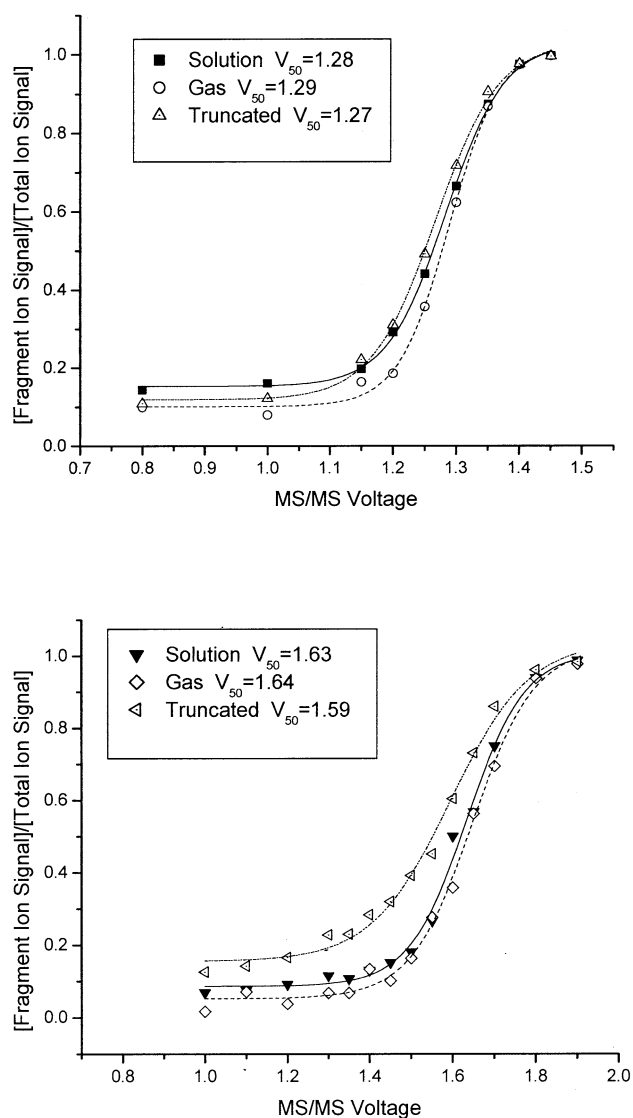Figure 5a shows the fragmentation energy plot for

Figure 5. (a) V_{50} plot of the fragmentation efficiency by ESI-QIT MS^n of the diacetylated solution-phase generated $[b_8 + OH + H]_S^+$ ion structural analog of bradykinin versus the diacetylated gas-phase generated $[b_8 + OH + H]^+$ ion of bradykinin vs. the diacetylated truncated *des*-Arg^9-bradykinin. (b) V_{50} plot of the fragmentation efficiency by ESI-QIT MS^n of the diacetylated solution-phase generated $[b_9 + OH + H]_S^+$ ion structural analog of angiotensin I vs. the diacetylated gas-phase generated $[b_9 + OH + H]^+$ ion of angiotensin I vs. the diacetylated truncated *des*-Leu^{10}-angiotensin I. The V_{50} plots for bradykinin are all superimposable; for angiotensin I, the V_{50} plot for the gas-phase generated $[b_9 + OH + H]^+$ ion and the solution-phase generated structural analog are identical, while the truncated angiotensin I fragments significantly more readily.

solution-phase generated $[b_8 + OH + H]_S^+$ ions structural analog of diacetylated bradykinin (peptide sequence RPPGFSPFR, m/z 988.5), gas-phase generated $[b_8 + OH + H]^+$ ions of diacetylated bradykinin (m/z 988.5), and truncated diacetylated *des*-Arg^9-bradykinin (m/z 988.5). The three plots are virtually identical, with V_{50} values of 1.28 ± 0.01 V and very similar curve shapes between the three species. These data strongly

suggest that the structures of the gas-phase generated and solution-phase generated $[b_8 + OH + H]^+$ ions are identical to the structure of the truncated *des*-Arg^9-bradykinin (i.e., loss of the C-terminal arginine and a free C-terminal carboxylic acid), which is in agreement with the MS/MS fragmentation spectra presented in Figure 3.

Figure 5b shows the fragmentation energy plot for solution-phase generated $[b_9 + OH + H]_S^+$ ion structural analogs of diacetylated angiotensin I (peptide sequence DRVYIHPFHL), gas-phase generated $[b_9 + OH + H]^+$ ions of diacetylated angiotensin I, and truncated diacetylated *des*-Leu^{10}-angiotensin I. The plots of solution-phase $[b_9 + OH + H]_S^+$ ion structural analogs and gas-phase generated $[b_9 + OH + H]^+$ ions are almost superimposable, with a V_{50} of 1.64 ± 0.01 V and virtually identical curve shapes. However, the plot of truncated *des*-Leu^{10}angiotensin I is significantly different from those of the gas-phase generated $[b_9 + OH + H]^+$ ions and solution-phase $[b_9 + OH + H]^+$ ion structural analogs, with a V_{50} significantly lower ($V_{50} = 1.59$). Due to the large number of spectra acquired, statistical analysis is difficult. One point chosen at random (*des*-Leu^{10-}angiotensin I at 1.65 V) was analyzed for statistical error, and was found to have a standard deviation of ± 0.010. These results agree nicely with the previous MS/MS spectra, which show the truncated diacetylated *des*-Leu^{10}-angiotensin I readily losing 60 Da from the amino acid side chains of arginine and aspartate (Fig 4c) while the gas-phase $[b_9 + OH + H]^+$ ions and solution-phase generated $[b_9 + OH + H]^+$ ion structural analogs fragmented primarily into the $[b_8 + OH + H]^+$ ion (Fig 4a-b). Combined with the MS/MS fragmentation pattern data, these results demonstrate that the structures of the $[b_9 + OH + H]^+$ ion and the $[b_9 + OH + H]_S^+$ ion structural analog of diacetylated angiotensin I is not the same as the diacetylated truncated *des*-Leu^{10}-angiotensin I. Higher energy MS/MS fragmentation experiments yielded sufficient fragment ions to show that the sites of acetylation of the diacetylated gas-phase $[b_9 + OH + H]^+$ ions, the diacetylated solution-phase $[b_9 + OH + H]_S^+$ ion structural analogs, and the diacetylated truncated *des*-Leu^{10}-angiotensin I all occurred at the same locations (N-terminus and Tyr^4); therefore, the structural difference almost certainly involves the C-terminus.

Previous MS/MS/MS experiments examining diacetylated angiotensin I found that the primary fragmentation pathway of the $[b_9 + OH + H]^+$ ion was loss of the C-terminal residue, resulting in the $[b_8 + OH + H]^+$ ion (Figure 4a). In order to test if this trend was observed with other specific-fragmenting peptides, we performed MS^n experiments on both solution-phase $[b_6 + OH + H]_S^+$ ion structural analogs and gas-phase formed $[b_6 + OH + H]^+$ ions of trifluoroacetylated Ile^7 angiotensin III (peptide sequence RVYIHPI, m/z 880.4). Figure 6a shows the MS^n spectra of trifluoroacetylated Ile^7 angiotensin III. The top panel is the MS^3 experiment; the base peak in this experiment is actually the
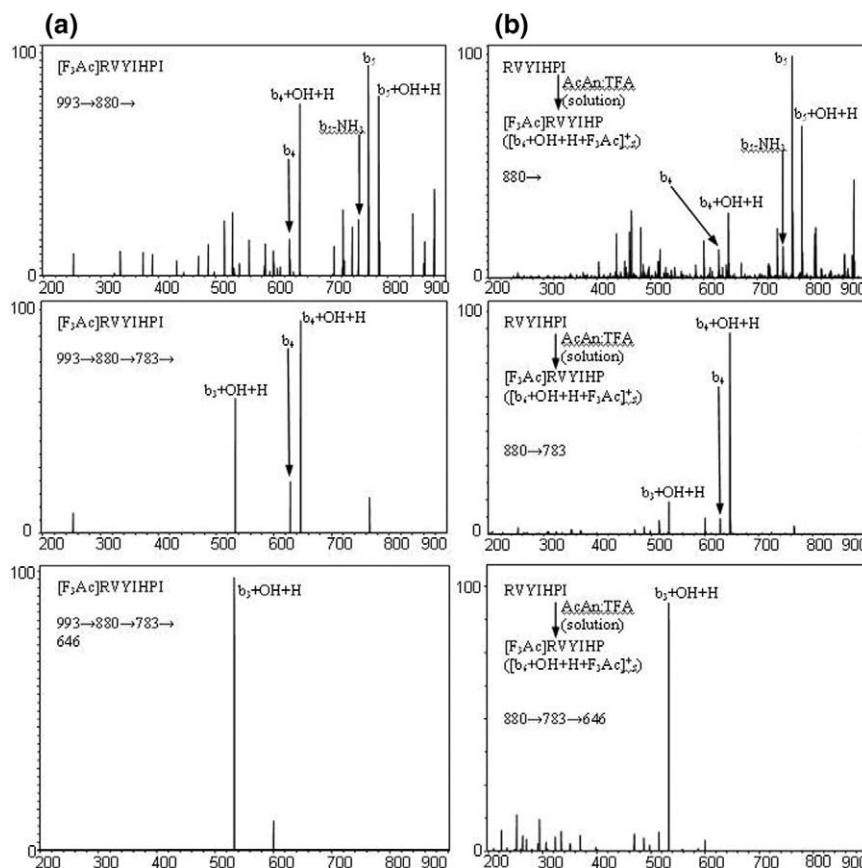
Figure 6. (**a**) ESI-QIT MS^n study of the fragmentation properties of the $[b_{(n-x)} + OH + H]^+$ ions of the gas-phase generated $[b_6 + OH + H]^+$ ion of N-terminally trifluoroacetylated Ile^7 angiotensin III. The top panel shows the fragmentation pattern of the $[b_6 + OH + H]^+$ ion of m/z 880 in an MS^3 experiment; the middle panel shows the fragmentation pattern of the $[b_5 + OH + H]^+$ ion of m/z 783 in an MS^4 experiment, and the bottom panel shows the fragmentation pattern of the $[b_4 + OH + H]^+$ ion of m/z 646 in an MS^5 experiment. (**b**) ESI-QIT MS^n study of the fragmentation properties of $[b_{(n-x)} + OH + H]^+$ ions of the solution-phase generated $[b_6 + OH + H]_S^+$ ion structural analog of N-terminally trifluoroacetylated Ile^7 angiotensin III. The top panel shows the fragmentation pattern of the $[b_6 + OH + H]_S^+$ ion structural analog of m/z 880 in an MS^2 experiment; the middle panel shows the fragmentation pattern of the $[b_5 + OH + H]^+$ ion of m/z 783 in an MS^3 experiment, and the bottom panel shows the fragmentation pattern of the $[b_4 + OH + H]^+$ ion of m/z 646 in an MS^4 experiment.

standard b$_5$ fragment ion. However, this may be attributable to the additional loss of water from the $[b_5 + OH + H]^+$ ion due to the characteristic nature of CAD in a quadrupole ion trap (multiple acceleration and deceleration events occurring over 40 ms in the presence of relatively high pressure helium), as fragmentation of the $[b_6 + OH + H]_S^+$ ion structural analogs by CAD on an ESI-Q-TOF hybrid instrument or by unimolecular decomposition on a MALDI-TOF-TOF instrument yield primarily the $[b_5 + OH + H]^+$ ion (data not shown).

The middle panel shows the MS^4 experiment, where the $[b_5 + OH + H]^+$ ion was isolated and fragmented. In this spectrum, the primary fragmentation product is the $[b_4 + OH + H]^+$ ion, although the overall signal has decreased due to ion loss in the MS^n process. In the bottom panel, an MS^5 experiment is shown, where the $[b_4 + OH + H]^+$ ion is isolated and fragmented. The primary product ion is the $[b_3 + OH + H]^+$ ion,

although there is very little overall signal. No further fragmentation could be accomplished due to a lack of signal in the MS^6 spectrum. Figure 6b shows an analogous experiment performed on the $[b_6 + OH + H]_S^+$ ion structural analog of trifluoroacetylated Ile^7 angiotensin III. The top panel shows the MS/MS spectrum of the $[b_6 + OH + H]_S^+$ ion structural analog. Again, the most abundant fragment ion is the b$_5$ ion due to the multiple collision mechanism of fragmentation in the QIT. The middle panel shows the MS^3 spectrum, where the $[b_5 + OH + H]^+$ ion was isolated and fragmented. The $[b_4 + OH + H]^+$ ion is the most abundant product of this fragmentation event. The bottom panel shows the MS^4 spectrum, where the $[b_4 + OH + H]^+$ ion was isolated and fragmented. Again, the peptide loses the C-terminal residue, retaining the C-terminal OH to form the $[b_3 + OH + H]^+$ ion. These data show that the specific-fragmentation occurs in an iterative fashion; therefore, the structure that promotes this specific-fragmentation
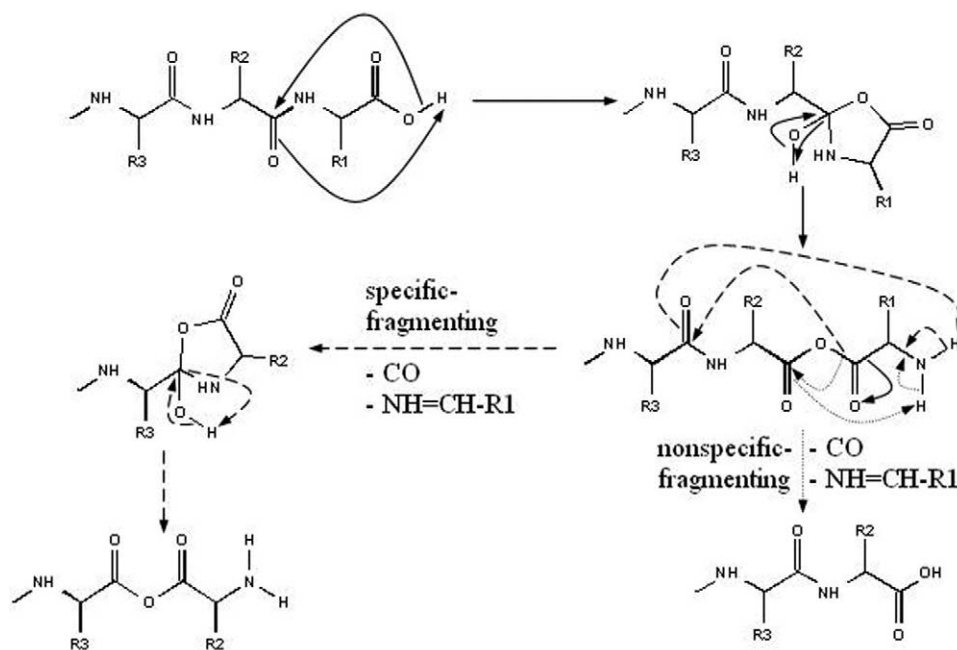
Scheme 3

in the $[b_{(n-1)} + OH + H]^+$ ion is probably retained in subsequent fragmentation and rearrangement events.

The nature of the chemistry itself for creating these solution-phase $[b_{(n-1)} + OH + H]^+_S$ ion structural analogs suggests certain ideas. The fact that these ions are generated in a reaction known to promote anhydride formation [24, 30] supports recent theoretical calculations that suggest that $[b_{(n-1)} + OH + H]^+$ and $[b_{(n-1)} + OH + Cat]^+$ ions go through an anhydride intermediate [16, 17]. However, all mechanisms for formation of $[b_{(n-1)} + OH + H]^+$ ions of which the authors are aware present a structure that is identical to the truncated peptide [12, 13, 16, 17]. Our results with using bradykinin, as well as by the work previously reported for bradykinin [22] support this structure for the $[b_{(n-1)} + OH + H]^+$ fragment ions; however, results for angiotensin I reported here directly refute this structure for these fragment ions. At least two different structures exist for $[b_{(n-1)} + OH + H]^+$ fragment ions, requiring different mechanisms of rearrangement and fragmentation.

One potential mechanism, based on the results presented here and the work reported by Farrugia and O'Hair on the fragmentation of arginine-containing dipeptides, [17] is proposed in Scheme 3. The portions that are marked with the heavy dashed lines are proposed for the specific-fragmenting peptides, while the portions of the mechanism represented by the dotted lines are consistent with the mechanisms previously reported [12, 13, 17] and consistent with the data reported here for nonspecific-fragmenting peptides. The portions of the mechanism represented by solid lines are shared between the two pathways. The proposed difference in the mechanisms of rearrangement

and fragmentation between the specific-fragmenting peptides and the nonspecific-fragmenting peptides hinge upon which carbonyl oxygen attacks the amine hydrogen at the C-terminal end of the peptide anhydride. For the specific-fragmenting peptides, the dominant rearrangement pathway results in a $[b_{(n-1)} + OH + H]^+$ ion that retains the linear anhydride structure. This retention of the linear anhydride structure promotes further fragmentation into the $[b_{(n-2)} + OH + H]^+$ ion upon subsequent activation events due to the fewer steps in the rearrangement process. For nonspecific-fragmenting peptides, the dominant fragmentation pathway results in a structure that is identical to the truncated peptide, making the formation of the $[b_{(n-2)} + OH + H]^+$ less likely, but still possible.

In order to determine if the structure proposed in Scheme 3 for the specific-fragmenting $[b_{(n-1)} + OH + H]^+$ ion is feasible, electron capture dissociation (ECD) was performed on the solution-phase formed, specific-fragmenting acetylated, trifluoroacetylated $[b_6 + OH + 2H]^{2+}_S$ ion structural analog of Ile^7 angiotensin III (peptide sequence RVYIHPI, m/z 922.5). ECD is a very rapid, nonergodic dissociation method [26]; therefore, the extensive rearrangements that occur during ergodic MS/MS processes (IRMPD, CAD) should not dominate the tandem mass spectrum, and more reliable information about the structure of the peptide should be obtainable. The ECD product spectrum for the solution-phase formed $[b_6 + OH + 2H + F_3Ac + Ac]^{2+}_S$ ion structural analog is shown in Figure 7. The fragments shown are consistent with the proposed structure for the specific-fragmenting $[b_{(n-1)} + OH + H]^+$ ion; however, the fragments do not rule out other structures for the C-terminus. The fragmentation pattern does
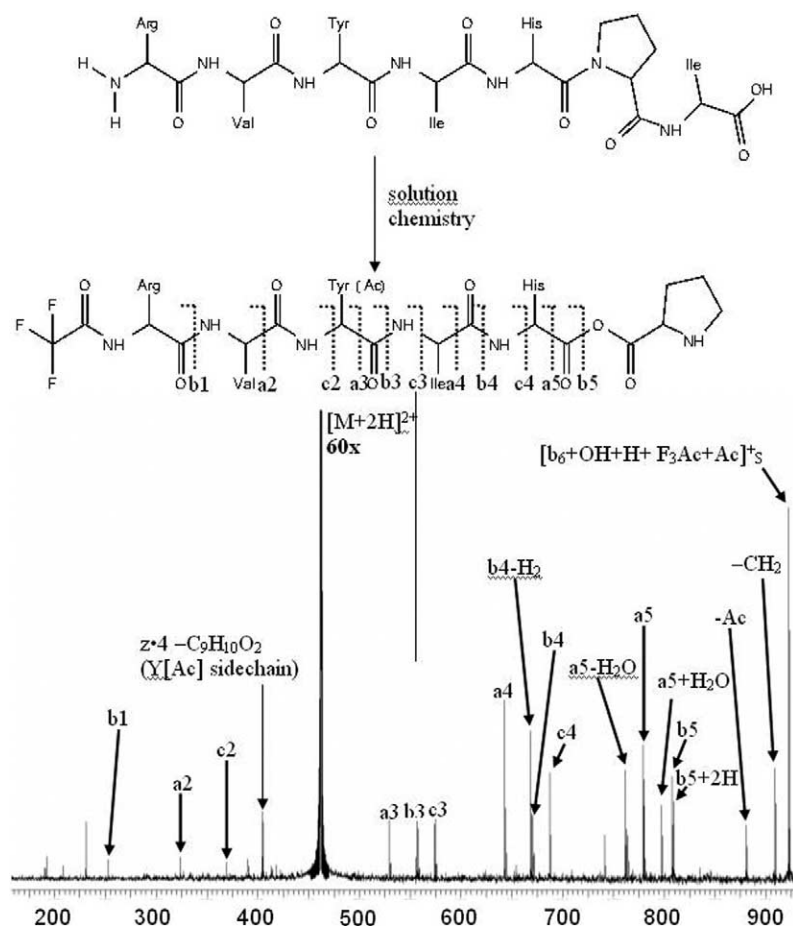
Figure 7. A comparison of the proposed structure of the specific-fragmenting acetylated, trifluoro-acetylated $[b_6 + OH + H]_S^+$ ion structural analog of Ile[7] angiotensin III and the ECD product spectrum of the solution-phase generated $[b_6 + OH + 2H]_S^{2+}$ ion structural analog of the specific-fragmenting acetylated, trifluoroacetylated Ile[7] angiotensin III.

clearly suggest that the rest of the peptide is unchanged; fragments from all along the backbone can be detected, showing that the structural differences must be at the C-terminus. The voltage used for generation of the electrons is near the border between traditional ECD and "hot" electron capture dissociation [31, 32], explaining the abundant secondary fragmentation ions resulting in the cleavage of almost every covalent bond along the backbone. Unfortunately, no bonds at the C-terminus were cleaved, preventing us from confirming or eliminating from consideration the structure for the $[b_{(n-1)} + OH + H]^+$ ion presented in Scheme 3.

Conclusions

The results of this study have led to a new tool in the study of the structure and properties of $[b_{(n-1)} + OH + H]^+$ ions, as well as a greater understanding of the nature of these ions. The data presented here have shown that solution-phase chemistry can generate peptide derivatives that are identical to gas-phase generated $[b_{(n-1)} + OH + H]^+$ ions. This discovery allows the researcher to bring an enormous array of analytical

techniques to bear on the question of the structure and properties of the $[b_{(n-1)} + OH + H]_S^+$ ion structural analog. Current efforts at purifying a solution-phase $[b_{(n-1)} + OH + H]_S^+$ ion structural analog of a specific-fragmenting peptide for analysis by NMR spectroscopy are underway. The results presented above show that at least two different structures exist for the $[b_{(n-1)} + OH + H]^+$ ion. One of these structures is probably identical to that of the corresponding truncated peptide (i.e., a free acid C-terminus). The other structure is clearly different. MS/MS fragmentation studies of $[b_{(n-1)} + OH + H]^+$ ions and their structural analogs that fragment identically to the truncated peptide show a fragmentation spectrum that does not particularly favor the formation of the $[b_{(n-2)} + OH + H]^+$ ion, while fragmentation studies of $[b_{(n-1)} + OH + H]^+$ ions and their structural analogs that do not fragment identically to the truncated peptide show a fragmentation spectrum that does favor the formation of the $[b_{(n-2)} + OH + H]^+$ ion. Analysis of the primary sequence of peptides in both groups failed to find any single structural feature that was common to only one group. Both the MS/MS fragmentation patterns and the measured V_{50} energy of

fragmentation show that one of these structures is almost certainly a free C-terminal carboxylic acid, identical to the truncated peptide. The other structure identified in this study is clearly different from the truncated peptide; however, the exact nature of this difference has not yet been determined. The observation that a structural analog which fragments identically to the $[b_{(n-1)} + OH + H]^+$ ion can be formed by chemical derivatization suggests that the structure of the $[b_{(n-1)} + OH + H]^+$ ion is not due to an intramolecular interaction within the peptide, but rather is due to a change in the covalently-bound structure. In addition, electron capture dissociation is known to usually preserve stable noncovalent bonds due to the nonergodic nature of the dissociation; therefore, the ECD experiment showed that the structural difference between specific-fragmenting $[b_{(n-1)} + OH + H]^+$ ions and the truncated peptide almost certainly occurs at the C-terminus. A potential mechanism for the formation of $[b_{(n-1)} + OH + H]^+$ ions has been presented; however, much more research must be performed before any mechanism for these rearrangement reactions can be relied upon with confidence. Examination of the structural differences between specific-fragmenting and nonspecific-fragmenting peptides (Table 2) does not yield any obvious structural causes for the differences in the dominant fragmentation pathway for each respective $[b_{(n-1)} + OH + H]^+$ ion. More study is required to determine why certain $[b_{(n-1)} + OH + H]^+$ ions fragment in a primarily specific fashion, while others fragment primarily nonspecifically. Continuing characterization of the solution-phase $[b_{(n-1)} + OH + H]_S^+$ ion structural analog using a variety of solution-phase analytical techniques such as NMR and FT-IR spectroscopy will allow the elucidation of the structure(s) of the $[b_{(n-1)} + OH + H]_S^+$ ion structural analog, which will greatly aid in the development of an accurate mechanism of formation.

References

1. Hunt, D. F.; Bone, W. M.; Shabanowitz, J.; Rhodes, J.; Ballard, J. M. Sequence-Analysis of Oligopeptides by Secondary Ion-Collision Activated Dissociation Mass-Spectrometry. *Anal. Chem.* **1981,** *53,* 1704–1706.

2. Wysocki, V. H.; Tsaprailis, G.; Smith, L. L.; Breci, L. A. Mobile and Localized Protons: A Framework for Understanding Peptide Dissociation. *J. Mass Spectrom.* **2000,** *35,* 1399–1406.

3. Schlosser, A.; Lehmann, W. D. Five-Membered Ring Formation in Unimolecular Reactions of Peptides: A Key Structural Element Controlling Low-Energy Collision-Induced Dissociation of Peptides. *J. Mass Spectrom.* **2000,** *35,* 1382–1390.

4. Polce, M. J.; Ren, D.; Wesdemiotis, C. Dissociation of the Peptide Bond in Protonated Peptides. *J. Mass Spectrom.* **2000,** *35,* 1391–1398.

5. Ambihapathy, K.; Yalcin, T.; Leung, H.; Harrison, A. G. Pathways to Immonium Ions in the Fragmentation of Protonated Peptides. *J. Mass Spectrom.* **1997,** *32,* 209–215.

6. Nold, M. J.; Wesdemiotis, C.; Yalcin, T.; Harrison, A. G. Amide Bond Dissociation in Protonated Peptides. Structures of the N-Terminal Ionic and Neutral Fragments. *Int. J. Mass Spectrom.* **1997,** *164,* 137–153.

7. Yalcin, T.; Csizmadia, I. G.; Peterson, M. R.; Harrison, A. G. The Structure and Fragmentation of Bn (n ≧ 3) Ions in Peptide Spectra. *J. Am. Soc. Mass Spectrom.* **1996,** *7,* 233–242.

8. Farrugia, J. M.; O'Hair, A. J.; Reid, G. E. Do All B2 Ions Have Oxazolone Structures? Multistage Mass Spectrometry and ab Initio Studies on Protonated *N*-Acyl Amino Acid Methyl Ester Model Systems. *Int. J. Mass Spectrom.* **2001,** *210/211,* 71–87.

9. Yalcin, T.; Khouw, C.; Csizmadia, I. G.; Peterson, M. R.; Harrison, A. G. Why are B Ions Stable Species in Peptide Spectra? *J. Am. Soc. Mass Spectrom.* **1995,** *6,* 1165–1174.

10. Yague, J.; Paradela, A.; Ramos, M.; Ogueta, S.; Marina, A.; Barahona, F.; Lopez de Castro, J. A.; Vazquez, J. Peptide Rearrangement During Quadrupole Ion Trap Fragmentation: Added Complexity to MS/MS Spectra. *Anal. Chem.* **2003,** *75,* 1524–1535.

11. Vachet, R. W.; Bishop, B. M.; Erickson, B. W.; Glish, G. L. Novel Peptide Dissociation: Gas-Phase Intramolecular Rearrangement of Internal Amino Acid Residues. *J. Am. Chem. Soc.* **1997,** *119,* 5481–5488.

12. Thorne, G. C.; Ballard, K. D.; Gaskell, S. J. Metastable Decomposition of Peptide [M + H]+ Ions via Rearrangement Involving Loss of the C-Terminal Amino Acid Residue. *J. Am. Soc. Mass. Spectrom.* **1990,** *1,* 249–257.

13. Gonzalez, J.; Besada, V.; Garay, H.; Reyes, O.; Padron, G.; Tambara, Y.; Takao, T.; Shimonishi, Y. Effect of the Position of a Basic Amino Acid on C-Terminal Rearrangement of Protonated Peptides Upon Collision-Induced Dissociation. *J. Mass Spectrom.* **1996,** *31,* 150–158.

14. Anbalagan, V.; Silva, A. T. M.; Rajagopalachary, S.; Bulleigh, K.; Talaty, E. R.; Van Stipdonk, M. J. Influence of "Alternative" C-Terminal Amino Acids on the Formation of [b3 + 17 + Cat]+ products from metal cationized synthetic tetrapeptides. *J. Mass Spectrom.* **2004,** *39,* 495–504.

15. Deery, M. J.; Summerfield, S. G.; Buzy, A.; Jennings, K. R. A Mechanism for the Loss of 60 u from Peptides Containing an Arginine Residue at the C-Terminus. *J. Am. Soc. Mass Spectrom.* **1997,** *8,* 253–261.

16. Feng, W. Y.; Gronert, S.; Fletcher, K. A.; Warres, A.; Lebrilla, C. B. The Mechanism of C-Terminal Fragmentations in Alkali Metal Ion Ccomplexes of Peptides. *Int. J. Mass Spectrom.* **2003,** *222,* 117–134.

17. Farrugia, J. M.; O'Hair, R. A. J. Involvement of Salt Bridges in a Novel Gas Phase Rearrangement of Protonated Arginine-Containing Dipeptides which Precedes Fragmentation. *Int. J. Mass Spectrom.* **2003,** *222,* 229–242.

18. Ballard, K. D.; Gaskell, S. J. Intramolecular [O-18] Isotopic Exchange in the Gas-Phase Observed During the Tandem Mass-Spectrometric Analysis of Peptides. *J. Am. Chem. Soc.* **1992,** *114,* 64–71.

19. Thorne, G. C.; Gaskell, S. J. Elucidation of Some Fragmentations of Small Peptides Using Sequential Mass Spectrometry on a Hybrid Instrument. *Rapid Commun. Mass Spectrom.* **1989,** *3,* 217–221.

20. Renner, D.; Spiteller, G. Linked Scan Investigation of Peptide Degradation Initiated by Liquid Secondary Ion Mass Spectrometry. *Biomed. Environ. Mass Spectrom.* **1988,** *15,* 75–77.

21. Tang, X. J.; Ens, W.; Standing, K. G.; Westmore, J. B. Daughter Ion Mass Spectra from Cationized Molecules of Small Oligopeptides in a Reflecting Time-of-Flight Mass Spectrometer. *Anal. Chem.* **1988,** *60,* 1791–1799.

22. Grese, R. P.; Cerny, R. L.; Gross, M. L. Metal-Ion Peptide Interactions in the Gas Phase—A Tandem Mass-Spectrometry Study of Alkali-Metal Cationized Peptides. *J. Am. Chem. Soc.* **1989,** *111,* 2835–2842.

23. Tomer, K. B.; Deterding, L. J.; Guenat, C. Collisionally Activated Dissociation Spectra of Sodiated Peptides and Peptide Amides. *Biol. Mass Spectrom.* **1991,** *20,* 121–129.

24. Hardeman, K.; Samyn, B.; Van der Eycken, J.; Van Beeumen, J. An Improved Chemical Approach Toward the C-Terminal Sequence Analysis of Proteins Containing All Natural Amino Acids. *Protein Sci.* **1998,** *7,* 1593–1602.

25. Senko, M. W.; Hendrickson, C. L.; Emmett, M. R.; Shi, S. D.-H.; Marshall, A. G. External Accumulation of Ions for Enhanced Electrospray Ionization Fourier Transform Ion Cyclotron Resonance Mass Spectrometry. *J. Am. Soc. Mass Spectrom.* **1997,** *8,* 970–976.

26. Zubarev, R. A.; Kelleher, N. L.; McLafferty, F. W. Electron Capture Dissociation of Multiply Charged Protein Cations. A Nonergodic Process. *J. Am. Chem. Soc.* **1998,** *120,* 3265–3266.

27. McLafferty, F. W.; Horn, D. M.; Breuker, K.; Ge, Y.; Lewis, M. A.; Cerda, B.; Zubarev, R. A.; Carpenter, B. K. Electron Capture Dissociation of Gaseous Multiply Charged Ions by Fourier-Transform Ion Cyclotron Resonance. *J. Am. Soc. Mass Spectrom.* **2001,** *12,* 245–249.

28. Tang, X. J.; Thibault, P.; Boyd, R. K. Fragmentation Reactions of Singly- and Doubly-Charged Alkali-Metal Ion-Peptide Complexes—A Reaction Specific to C-Terminal Arginine Residues. *Org. Mass Spectrom.* **1993,** *28,* 1047–1052.

29. Dongre, A. R.; Jones, J. L.; Somogyi, A.; Wysocki, V. H. Influence of Peptide Composition, Gas-Phase Basicity, and Chemical Modification on Fragmentation Efficiency: Evidence for the Mobile Proton Model. *J. Am. Chem. Soc.* **1996,** *118,* 8365–8374.

30. Kubo, H.; Nakajima, T.; Tamura, Z. Formation of Thiohydantoin Derivative of Proline from C-Terminal of Peptides. *Chem. Pharm. Bull.* **1971,** *19,* 210–211.

31. Kjeldsen, F.; Haselmann, K. F.; Budnik, B. A.; Jensen, F.; Zubarev, R. A. Dissociative Capture of Hot (3–13 eV) Electrons by Polypeptide Polycations: An Efficient Process Accompanied by Secondary Fragmentation. *Chem. Phys. Lett.* **2002,** *356,* 201–206.

32. Haselmann, K. F.; Budnik, B. A.; Kjeldsen, F.; Nielsen, M. L.; Olsen, J. V.; Zubarev, R. A. Electronic Excitation Gives Informative Fragmentation of Polypeptide Cations and Anions. *Eur. J. Mass Spectrom.* **2002,** *8,* 117–121.